Dissimilar joining of molybdenum to tungsten and graphite using Cu78Ti22 filler

Longkun Huang[1], Siyu Miao[1], Yingjie Zeng[1], Yuqi Cai[1], Julfikar Haider[2], Yangwu Mao[1,3,*]

[1] Hubei Key Laboratory of Plasma Chemistry and Advanced Materials, Wuhan Institute of Technology, Wuhan 430205, China

[2] Department of Engineering, Manchester Metropolitan University, Manchester M1 5GD, UK

[3] Key Laboratory of Green Chemical Engineering Process of Ministry of Education, Wuhan Institute of Technology, Wuhan 430205, China

* Corresponding author, Email: myw@wit.edu.cn

Tel: +86-27-87195661 Fax: +86-27-87195661

Abstract

Brazing of molybdenum to tungsten and to graphite has been achieved using Cu78Ti22 filler at 930℃. The brazing regions of both joints are mainly composed of Cu(ss) (solid solution), Ti-Cu intermetallics, Ti(ss) and Mo. The diffusion and dissolution of Mo element from the molybdenum substrate to the brazing region occur during the joining process for both joints. For the molybdenum/tungsten joint, the absorption of Ti on the tungsten side may promote interfacial bonding between the brazing region and the tungsten substrate. For the molybdenum/graphite joint, the active Ti in the filler can react with the graphite to develop a reaction layer of TiC at the brazing region/graphite interface, contributing to the interfacial bonding between the brazing region and the graphite. The fracture of the molybdenum/tungsten joint after the shear test occurs at the brazing region/tungsten interface, which is attributed to its relatively weak interfacial bonding. The molybdenum/graphite joint breaks on the graphite side, mainly caused by the large residual stress in the joint.

Keywords

Brazing · Molybdenum · Tungsten · Graphite · Microstructure

1 Introduction

Molybdenum is broadly used in the electronics, medical and nuclear industries due to its outstanding mechanical and thermal properties [1]. However, many practical applications involve combining molybdenum with other materials. For example, manufacturing the hot cathode in a microwave tube requires the joining of molybdenum with tungsten [2]. Fabrication of the X-ray anode target in a high-power computed tomography device involves

the joining of molybdenum with graphite [3]. Therefore, molybdenum/tungsten and molybdenum/graphite joining are of great significance for industrial applications.

Joining techniques such as diffusion bonding [4], electron beam welding [5], laser welding [6], vacuum arc pressure brazing [7] and brazing [2, 8-16] have been used to join molybdenum to other materials. Brazing is preferred for dissimilar materials joining due to its ease of processing, high reliability, low damage to the substrates and low cost [17, 18]. The brazes used in molybdenum/other material brazing include Ni-, Ti- and Pd-based fillers. Min et al. [8] and Xu et al. [2] brazed molybdenum to other materials (including 316L steel, tungsten and graphite) at 1060℃ using BNi2 (NiCrSiBFe) filler. Microstructural characterization revealed that a diffusion layer containing Mo and MoNi formed close to the molybdenum substrate. Wang et al. [9] brazed molybdenum to C/C composite at 1330℃ using BNi5 (NiCrSi) + 5% Ti filler. The results showed that MoNiSi and Ni(ss) (solid solution) developed in the joining region, which could reduce the joint residual thermal stress by the plastic deformation of Ni(ss). Sene and Motta [10] studied molybdenum/porous tungsten brazing with Ni62Mo38 filler at 1400℃. The results showed that the $MoNi_4$ phase was created in the brazing region. Fedotov et al. [11] brazed molybdenum to graphite at 1400℃ using Ti50Zr40Nb8.5Be1.5 filler. The brazing region was composed of β-(Ti,Mo)(ss), ZrC, $TiBe_2$, $MoBe_2$ and TiC. Liu et al. [12] performed molybdenum alloy/graphite brazing using Ti60Cr40 filler at 1480℃. The microstructure of the joint was molybdenum alloy/Ti-Mo(Cr)/Ti-Cr(Mo)/TiC/Cr_3C_2/graphite. Lu et al. [13] conducted molybdenum alloy/graphite brazing using Ti-containing fillers such as Ti67Cr33, Ti91.5Si8.5 and Ti67V30Mo3 at 1300–1700℃. The results showed that (Ti,Mo)(ss) was developed at the interface between the molybdenum alloy and the brazing region. Lin et al. [14] brazed molybdenum/porous tungsten using Ti foil at 1680–1740℃ and Pd foil at 1580–1640℃. The results showed that the Ti-rich melt infiltrated into the porous tungsten, resulting in poor bonding for the joint with the Ti foil. Feng et al. [15] and Lin et al. [16] carried out molybdenum/SiC brazing with AuPdCoMnNi high-entropy alloy filler at 1150℃ and FeCoCrNi high-entropy alloy filler at 1320–1480℃, respectively. However, numerous micro-cracks existed in the joint with AuPdCoMnNi filler.

Although the study of brazing molybdenum to other materials has been explored, there are still some issues concerning fillers. First, the brazing temperature for Ni-, Ti-, Pd-based and high-entropy alloy fillers used in molybdenum/other material brazing is relatively high (1060–1400℃ for Ni-based fillers [2, 8-10], 1300–1700℃ for Ti-based fillers [11-13], 1610℃ for Pd foil [14], and 1150–1480℃ for high-entropy alloys [15, 16]). Second, the Pd- and Au-containing fillers (Pd foil used in molybdenum/porous tungsten brazing and AuPdCoMnNi filler used in molybdenum/SiC brazing) are expensive because of the high cost of Pd and Au. Third, the

Ti50Zr40Nb8.5Be1.5 filler used in molybdenum/graphite brazing is harmful due to the presence of toxic Be. Therefore, developing a non-toxic filler with a low brazing temperature and low cost for brazing molybdenum/other materials is critical.

Given that Cu has a relatively low brazing temperature and is a cost-effective material, Cu-based filler may be a promising option for molybdenum/tungsten and molybdenum/graphite brazing. On the basis of the Cu-Ti phase diagram [19], a Cu-Ti eutectic phase can be formed at 875℃ when the weight ratio of Cu-Ti is 78:22. Additionally, the active metal Ti may be beneficial for the wetting of Cu-based filler on graphite because of its high chemical affinity with graphite. Thus, Cu78Ti22 (containing 78 wt% Cu and 22 wt% Ti) filler was used in this study for molybdenum/tungsten and molybdenum/graphite brazing. The microstructures and mechanical properties of the joints were characterized.

2 Materials and methods

Pure molybdenum (density: 10.2 g/cm^3, purity: 99.9%, size: 10 × 10 × 3 mm^3), pure tungsten (density: 19.2 g/cm^3, purity: 99.9%, size: 10 × 10 × 5 mm^3) and graphite (density: 1.9 g/cm^3, purity: 99.9%, size: 10 × 10 × 10 mm^3) substrates were purchased from Dongguan Shengze Metal Materials Co., China, Xingtai Jinou Metal Materials Co., China, and Jinglong Carbon Co., Beijing, China, respectively. The joining surfaces (10 × 10 mm^2) of the substrates were treated with sandpaper to remove impurities and then ultrasonically cleaned in deionized water for 20 minutes and in ethanol for another 20 minutes.

The Cu78Ti22 filler consisted of 78 wt.% Cu and 22 wt.% Ti. To avoid oxidation of Ti, TiH_2 powder was used to replace Ti. Both the Cu powders (size: -500 mesh; purity: 99.5%) and TiH_2 powders (size: -300 mesh; purity: 99.5%) were purchased from Xingrongyuan Co., Beijing, China. The Cu78Ti22 filler was prepared by mixing powders of Cu and TiH_2 at a weight ratio of 78:22. The micrograph of the Cu78Ti22 powder filler is shown in Fig. 1a. The spherical Cu powders and irregular TiH_2 powders can be observed in the mixed powder filler. Then, organic solvents were mixed with the Cu78Ti22 powder filler to obtain a paste with favorable flowability and viscosity. Notably, the brazing temperature is generally 50~100℃ higher than the melting temperature of the filler. The melting temperature of eutectic Cu78Ti22 alloy is 875℃ according to the Cu-Ti phase diagram [19]. Therefore, the brazing temperature for molybdenum/tungsten and molybdenum/graphite brazing with Cu78Ti22 filler was determined to be 930℃.

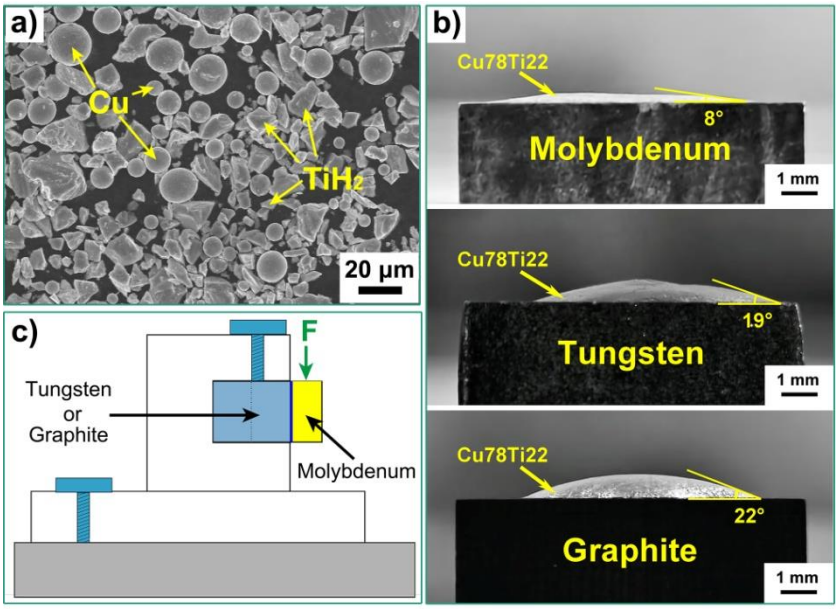

Fig. 1 a Micrograph of the Cu78Ti22 powder filler, **b** Wetting picture of the Cu78Ti22 filler on three substrates, and **c** Schematic of shear strength tests for molybdenum/tungsten and molybdenum/graphite joints

Before brazing, wetting experiments of the Cu78Ti22 filler on the molybdenum, tungsten and graphite substrates were conducted at 930℃ for 10 min. The wetting picture of the molten Cu78Ti22 filler on three substrates is shown in Fig. 1b. The contact angles of the molten Cu78Ti22 filler on the molybdenum, tungsten and graphite substrates are 8°, 19°, and 22°, respectively, indicating favorable wetting of the Cu78Ti22 filler on the three substrates.

Brazing of molybdenum to tungsten and to graphite was conducted in a molybdenum filament oven under a vacuum of 6.0×10^{-3} Pa. The Cu78Ti22 filler paste was coated on the brazing surfaces of the substrates. The substrates coated with the filler paste were assembled to form a sandwich structure (molybdenum/Cu78Ti22 filler/tungsten and molybdenum/Cu78Ti22 filler/graphite). The brazing assemblies were loaded with a pressure of 4.7 kPa to facilitate intimate contact of the filler with the substrates. The assemblies were heated to 500℃ (heating rate: 10℃/min) from room temperature and then held at 500℃ for 30 minutes to completely volatilize the organic solvents in the Cu78Ti22 filler paste. The assemblies were subsequently heated to 700℃ (heating rate: 10℃/min) and held at 700℃ for 30 minutes to ensure complete decomposition of the TiH_2 in the filler. The assemblies were heated to 930℃ (heating rate: 5℃/min) and held for 10 minutes. Afterwards, the assemblies were cooled to room temperature inside the oven via the oven cooling.

Field emission scanning electron microscopy (FESEM, GeminiSEM 300) was used to characterize the microstructure of the interface region in the molybdenum/tungsten and molybdenum/graphite joints. Energy

dispersive spectroscopy (EDS, Oxford Inca X-Act) was employed to characterize the elemental composition of the corresponding region. A Vickers hardness tester (HXD-1000TMC/LCD) was employed to measure the microhardness of the molybdenum/tungsten and molybdenum/graphite joints. The microhardness was determined with a load of 0.98 N and a dwell time of 10 s. At least three similar regions were tested to obtain the average microhardness of the joints. The shear strengths of the joints were determined by measurements described elsewhere [20]. The schematic of the shear strength test is shown in Fig. 1c. The average joint strength was calculated on the basis of at least three samples made with the same brazing parameters.

3 Results and discussion

3.1 Molybdenum/tungsten joint microstructure

Fig. 2 displays the micromorphology and EDS mappings of the molybdenum/tungsten joint with Cu78Ti22 filler. Neither pores nor cracks are observed at the molybdenum/brazing region and brazing region/tungsten interfaces, indicating favorable interfacial bonding in the molybdenum/tungsten joint. The brazing region, which is approximately 150 μm thick, consists of grey regions and dark-grey block regions. In addition, a small number of light-grey granular regions are distributed in the brazing region close to the molybdenum side, indicating Mo dissolution from the molybdenum substrate into the brazing region. The EDS mappings shown in Fig. 2b–e reveal that the Cu and Ti are present mainly in the brazing region. However, the Cu element is enriched in the grey region, whereas the Ti element is concentrated in the dark-grey region. Furthermore, W element is not observed in the brazing region, suggesting negligible diffusion of W from the tungsten substrate to the brazing region.

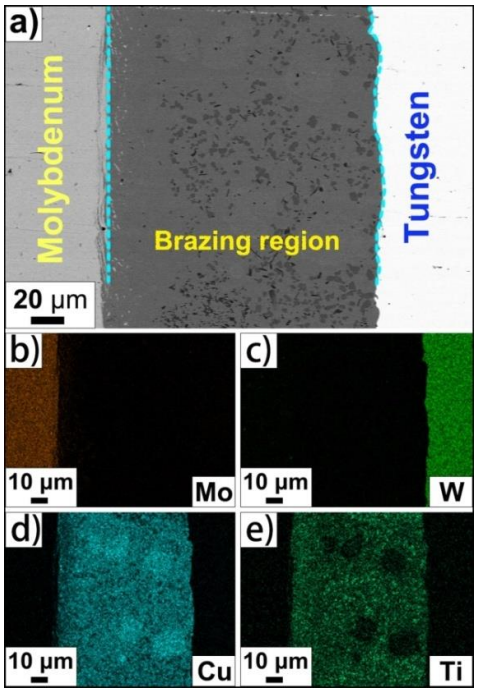

Fig. 2 a Micromorphology and **b-e** EDS mappings of the molybdenum/tungsten joint with Cu78Ti22 filler

The enlarged SEM images of the molybdenum/tungsten joint are shown in Fig. 3. It can be clearly seen in Fig. 3a that a small number of white regions exist in the brazing region adjacent to the molybdenum substrate. Table 1 lists the composition results of the microregions in Fig. 3 characterized by EDS. The EDS result of white microregion A near the molybdenum substrate shows that it contains 95.02 at% Mo, confirming the diffusion and dissolution of the molybdenum substrate into the brazing region. Liu et al. [21] pointed out that the Mo-Cu system exhibited negligible mutual solubility at temperature lower than 1084℃. Lin et al. [22] claimed that both the diffusion and dissolution of Mo from molybdenum into the brazing region were caused by the existence of Ti in the filler in molybdenum/molybdenum brazing with Ti60Ni25Nb15 filler. Thus, the existence of Ti in the filler results in the Mo diffusion into the brazing region.

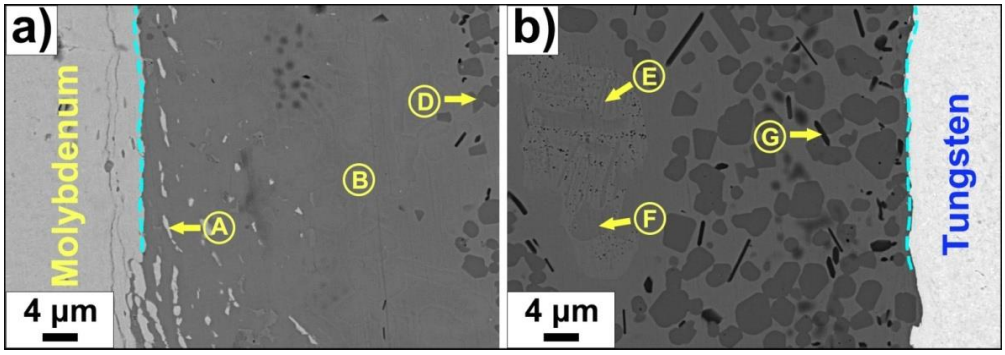

Fig. 3 Enlarged images of the interfacial region in the molybdenum/tungsten joint with Cu78Ti22 filler: **a** Molybdenum/brazing region side and **b** Brazing region/tungsten side

Table 1 EDS results of the microregions marked in Fig. 3

Microregions	Mo (at. %)	W (at. %)	Cu (at. %)	Ti (at. %)	Possible phases
A	95.02	-	3.23	1.75	Mo
B	0.21	-	51.23	48.56	TiCu
D	0.81	-	38.26	60.93	Ti_2Cu
E	0.10	-	93.87	6.03	Cu(ss)
F	0.12	-	79.07	20.81	$TiCu_4$
G	-	-	8.05	91.95	Ti(ss)

The grey microregion B contains 51.23 at.% Cu and 48.56 at.% Ti. The Ti/Cu atomic ratio is close to 1:1, presumably determined as TiCu intermetallics. Liu et al. [21] identified TiCu intermetallics in the joining region of molybdenum/copper joint diffusion bonded with Ti foil. For microregion D in the dark-grey block region and microregion F in the grey region, the Ti/Cu atomic ratios are approximately 2:1 and 1:4, respectively. Consequently, they are speculated to be Ti_2Cu and $TiCu_4$. The light-grey microregion E shows high Cu content (93.87 at.%), inferred predominantly as Cu(ss). Peng et al. [23] reported that the brazing region in the tungsten/copper alloy joint with Cu78Ti22 filler was composed of Ti_2Cu, $TiCu_4$ and Cu(ss), which is similar to the results of this study. The following reactions can take place in the Cu-Ti filler [24, 25]:

$$Ti + Cu = TiCu \qquad \Delta G\ (J/mol) = -17069 + 4.887\ T \tag{1}$$

$$2Ti + Cu = Ti_2Cu \qquad \Delta G\ (J/mol) = -36393 + 14.06\ T \tag{2}$$

$$Ti + 4Cu = TiCu_4 \qquad \Delta G\ (J/mol) = -30055 + 11.70\ T \tag{3}$$

The calculated ΔG (change in Gibbs free energy) values for reactions (1), (2) and (3) at 1203 K are –11.190 kJ/mol, –19.479 kJ/mol and –15.980 kJ/mol, respectively, indicating the possibility of Ti-Cu intermetallic formation in the brazing region.

Furthermore, the black whisker-like microregion G near the tungsten substrate contains a high Ti composition (91.95 at.%), which is assumed to be Ti(ss). Duan et al. [20] also detected Ti(ss) in the brazing region of the graphite/Ti6Al4V joint using Cu78Ti22 filler.

It is worth noting that the Mo element is detected in microregions B~F in the brazing region, confirming that Mo diffuses from the molybdenum substrate to the brazing region during the joining process. In contrast, W is not detected in the brazing region, suggesting negligible diffusion of W from the tungsten substrate to the

brazing region. Izaguirre et al. [26] claimed that no diffusion or interfacial reaction was involved in tungsten/Cu interface for tungsten/Eurofer steel brazing with a Cu interlayer at 1110℃. de Prado et al. [27] reported that neither diffusion nor dissolution of W occurred between the tungsten substrate and Cu80Ti20 filler in tungsten/Eurofer steel brazing with Cu80Ti20 filler at 950℃. Shang et al. [28] demonstrated that the absorption of active Ti on tungsten in tungsten/Fe-Ni-Co alloy brazing with Ag69.5Cu27Ti3.5 filler could cause the liquid filler to spread and dissolve on the tungsten substrate. This absorption resulted in improved interfacial bonding between the liquid filler and the tungsten substrate. Considering that the brazing temperature of 930℃ is employed in this study, no mutual diffusion takes place between the tungsten and the Cu78Ti22 filler. Nevertheless, the active Ti in the filler may be adsorbed on the tungsten side, thereby promoting the bonding of the brazing region with the tungsten substrate.

Microstructure characterization reveals that in molybdenum/tungsten brazing with Cu78Ti22 filler, diffusion and dissolution of the molybdenum substrate into the liquid filler occur. This can lead to strong metallurgical bonding between the molybdenum substrate and the brazing region. However, neither diffusion nor dissolution occurs between the tungsten and the Cu78Ti22 filler. Only the active Ti in the liquid filler may be adsorbed on the tungsten side, promoting interfacial bonding between the brazing region and the tungsten substrate.

3.2 Molybdenum/graphite joint microstructure

Fig. 4 shows the micromorphology and EDS mappings of the molybdenum/graphite joint with Cu78Ti22 filler. As revealed in Fig. 4a, a satisfactory interfacial bonding is achieved in the joint. The brazing region consisting of grey and dark-grey areas exhibits a thickness of about 110 μm, which is less than that of the molybdenum/tungsten joint with Cu78Ti22 filler (about 150 μm). This may be due to penetration of the molten filler into the porous graphite. Additionally, similar to the molybdenum/tungsten joint, a small number of white areas can be observed in the brazing region close to the molybdenum substrate, indicating the diffusion and dissolution of the molybdenum substrate into the brazing region.

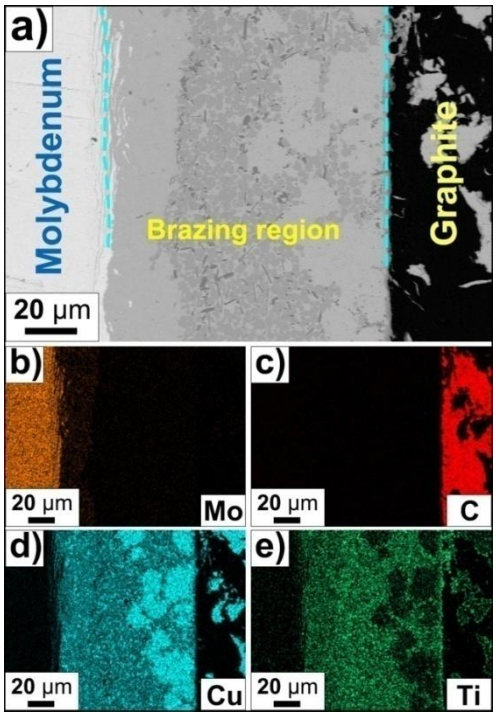

Fig. 4 a Micromorphology and **b-e** EDS mappings of the molybdenum/graphite joint with Cu78Ti22 filler

The EDS mappings in Fig. 4b–e indicate that the brazing region comprises Cu and Ti along with a small quantity of Mo. Moreover, Cu is abundant in the grey area, whereas Ti is present mainly in the dark-grey area. Furthermore, enrichment of the Ti element is observed at the brazing region/graphite interface due to the strong chemical affinity of Ti with graphite, which implies the development of a TiC layer near the graphite. In particular, the EDS maps of Ti and Cu shown in Fig. 4d–e reveal the presence of Ti and Cu inside the graphite, indicating the infiltration of the Cu78Ti22 molten filler into the porous graphite. This infiltration can not only increase the density and strength of the graphite substrate but also contribute to the interfacial bonding of the brazing region with the graphite substrate [29].

The magnified images of the interfacial region in the molybdenum/graphite joint are displayed in Fig. 5. The EDS results of the highlighted microregions are listed in Table 2. Dark-grey microregion A contains 64.13 at.% Ti and 35.67 at.% Cu (the atomic ratio of Ti/Cu is approximately 2:1), which can be speculated to be Ti_2Cu. The Ti/Cu atomic ratios of grey microregions B and F are approximately 1:1 and 1:4, respectively, corresponding to TiCu and $TiCu_4$.

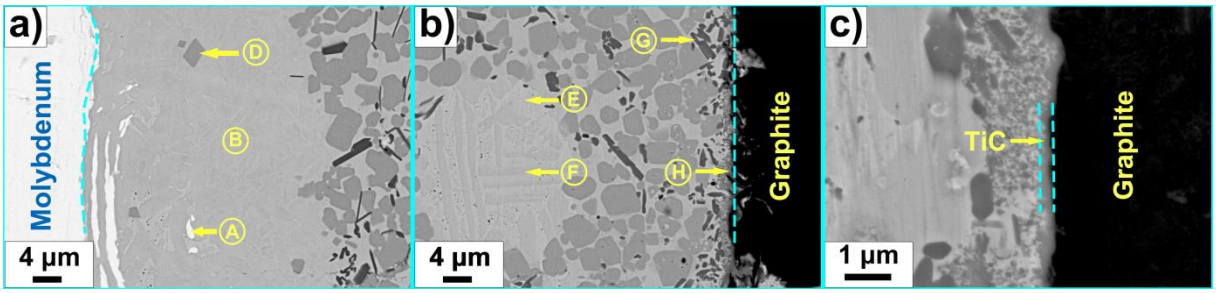

Fig. 5 Magnified images of the interfacial region in the molybdenum/graphite joint with Cu78Ti22 filler: **a** Molybdenum/brazing region side, **b** Brazing region/graphite side, and **c** Enlarged brazing region/graphite interface

Table 2 EDS results of the microregions in Fig. 5

Microregions	Ti (at. %)	Cu (at.%)	Mo (at.%)	C (at.%)	Possible phases
A	64.13	35.67	0.20	-	Ti_2Cu
B	44.80	54.11	1.09	-	TiCu
D	0.95	0.19	98.86	-	Mo
E	3.04	96.70	0.26	-	Cu(ss)
F	21.82	78.08	0.10	-	$TiCu_4$
G	92.36	6.62	1.02	-	Ti(ss)
H	50.97	2.40	0.31	46.32	TiC

The white microregion D shows a high Mo content (98.86 at.%), confirming the diffusion and dissolution of the molybdenum substrate into the brazing region. The light-grey microregion E and black whisker-like microregion G comprise high Cu content (96.70 at.%) and high Ti content (92.36 at.%), determined as Cu(ss) and Ti(ss), respectively. The microregion H in the dark-grey continuous layer near the graphite shows the Ti/C atomic ratio of approximately 1:1, suggesting the formation of a TiC layer at the brazing region/graphite interface. As shown in Fig. 5c, the thickness of the TiC reaction layer is about 200 ~ 300 nm. Vidyuk et al. [30] reported the formation of a TiC layer with a thickness of about 0.5–1 μm at the graphite/filler interface in graphite/Cu joint with Cu75Ti25 filler. Song et al. [31] also illustrated the formation of TiC layer in the carbon-carbon composite/Ti6Al4V alloy joint using Ti57Cu23Zr11Ni9 filler. They claimed that the TiC layer was beneficial for promoting the joint strength.

As proposed by Shi et al. [32], the following reaction can occur:

$$Ti + C = TiC \qquad \Delta G\ (J/mol) = -183050 + 10.083T \qquad (4)$$

The ΔG value for reaction (4) at 930℃ is –195.18 kJ/mol, indicating the feasibility of TiC formation at the brazing region/graphite interface in molybdenum/graphite brazing with Cu78Ti22 filler.

According to the microstructural analyses, for molybdenum/graphite brazing with Cu78Ti22 filler, favorable interfacial bonding between the molybdenum and the brazing region is achieved by the diffusion and dissolution of the molybdenum, similar to that in molybdenum/tungsten brazing with Cu78Ti22 filler. The satisfactory interfacial bonding between the graphite and the brazing region is attributed to the formation of the TiC reaction layer due to the reaction of the Ti in the filler with the graphite.

3.3 Mechanical properties of joints

Fig. 6 shows microhardness distributions of the molybdenum/tungsten and molybdenum/graphite joints. The hardness of the graphite is not shown, as it is difficult to distinguish the size of the indentation for the black graphite. The microhardness values of the molybdenum substrates in the molybdenum/tungsten and molybdenum/graphite joints are 280 ± 16 $HV_{0.1}$ and 292 ± 16 $HV_{0.1}$, respectively. This is in agreement with the value (290 HV) reported by Zhou et al. [33] in molybdenum/tantalum laser joining with Ni filler. The hardness of tungsten in the molybdenum/tungsten joint is 594 ± 14 $HV_{0.1}$, close to the hardness (560 HV) reported by Manikandan et al. [34] in tungsten/copper explosive welding. As demonstrated by Bonk et al. [35], the microhardness of tungsten depended significantly on its grain size (390 HV, 450~500 HV, 500~650 HV and 650~700 HV corresponded to single-crystal, coarse, fine and ultrafine grain types, respectively). Thus, the microhardness of the tungsten in this study implies that the tungsten belongs to the fine-grain type.

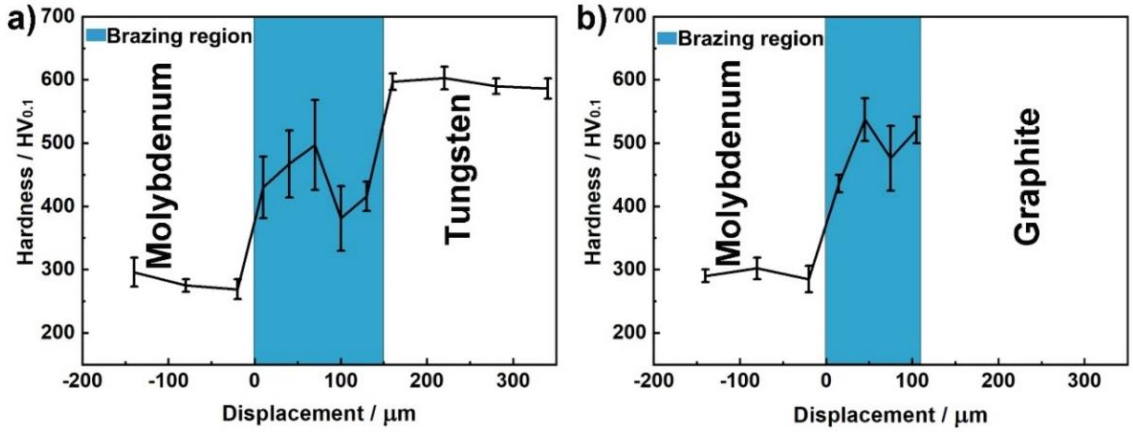

Fig. 6 Microhardness distributions of **a** molybdenum/tungsten and **b** molybdenum/graphite joints

The microhardness values of the brazing regions in the molybdenum/tungsten and molybdenum/graphite

joints exhibit considerable variation (with average microhardness of 438 ± 59 $HV_{0.1}$ and 493 ± 33 $HV_{0.1}$, respectively). As revealed by the microstructural characterization of the joints, the brazing regions in both the molybdenum/tungsten and molybdenum/graphite joints are mainly composed of TiCu, Ti_2Cu, $TiCu_4$, Ti(ss), Cu(ss) and Mo. Therefore, the microhardness of the various regions may result in significant variation in the brazing region. Chu et al. [36] reported that the hardness values of Cu(ss) and TiCu were 126 HV and 415 HV respectively. The microhardness values of Ti_2Cu, $TiCu_4$, Ti(ss) and Mo were found to be 508 HV [37], 573 HV [19], 342 HV [38], and 290 HV [33], respectively. The microhardness values of the brazing regions (438 $HV_{0.1}$ and 493 $HV_{0.1}$) in the molybdenum/tungsten and molybdenum/graphite joints in this study fall within the range of 126–573 HV. Thus, the microhardness results of the brazing regions in the molybdenum/tungsten and molybdenum/graphite joints are highly related to their microstructures. Notably, the brazing region in the molybdenum/graphite joint shows a slightly higher hardness than that in the molybdenum/tungsten joint. Given the high hardness of TiC, the development of the TiC layer near the graphite side may result in a slight hardness increase in the brazing region of the molybdenum/graphite joint.

Fig. 7 shows the shear strength and displacement-load curves of the molybdenum/tungsten and molybdenum/graphite joints as well as their fracture images. The shear strength of the molybdenum/tungsten joint is 51.4 ± 7.3 MPa, close to that of the tungsten/Eurofer alloy joint with Cu80Ti20 filler (55–92 MPa) [39]. Fracture of the molybdenum/tungsten joint after the shear test occurs at the brazing region/tungsten interface, as shown in Fig. 7c. As revealed by the microstructural analysis of the joint, there is no diffusion or dissolution between the tungsten and the filler. Only Ti absorption on the tungsten surface promotes interfacial bonding. As a result, the interfacial bonding between tungsten and the brazing region is relatively weak compared with that between molybdenum and the brazing region. de Prado et al. [40] reported that owing to the weak bonding in tungsten/steel brazing with Cu80Ti20 filler, joint fracture occurred at the tungsten/brazing region interface, similar to the fracture behavior in this study.

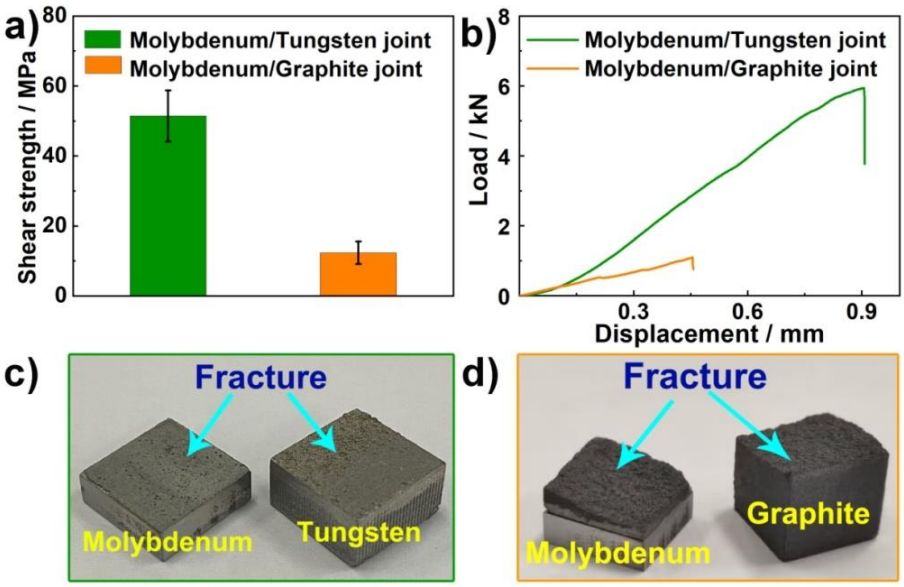

Fig. 7 **a** Shear strength and **b** displacement-load curves of molybdenum/tungsten and molybdenum/graphite joints; Fracture images of **c** molybdenum/tungsten and **d** molybdenum/graphite joints after shearing tests

The molybdenum/graphite joints exhibit the shear strength of 12.3 ± 3.2 MPa, reaching 80.9% of the graphite strength (15.2 ± 1.4 MPa, measured with the graphite size of 10 × 10 × 20 mm^3). This indicates strong interfacial bonding in molybdenum/graphite brazing with Cu78Ti22 filler. Dong et al. [7] reported that the shear strength of the molybdenum/graphite joint with Ti50Zr50 filler was 15.2 MPa, which was slightly higher than that obtained in this study. However, the high pressure (0.3–0.5 MPa) and high brazing temperature for the Ti-Zr filler required in their study may result in a high cost compared with that in this study. The fracture of the molybdenum/graphite joint after the shearing test displayed in Fig. 7d indicates that the joint breaks on the graphite close to the brazing region, which may be caused by the large residual stress in the joint. Considering that there is a large difference in the coefficient of thermal expansion among molybdenum, Cu78Ti22 filler and graphite (5.0 × 10^{-6}/℃, 10.9–13.5 × 10^{-6}/℃ and 0.6–4.3 × 10^{-6}/℃ [2,41,42], respectively), a large stress concentration is generated on the graphite side during the cooling process after high-temperature brazing. Xing et al. [43] demonstrated that bowl-shaped fracture suggested the existence of joint residual stress in graphite/Cu joining with Ti foil. Thus, the bowl-shaped fracture in the molybdenum/graphite joint shown in Fig. 7d also confirms that the fracture is caused by the large residual stress in the joint.

4 Conclusions

(1) Brazing of molybdenum to tungsten and graphite has been achieved using Cu78Ti22 filler at 930℃ for 10

min. The brazing regions of both joints are mainly composed of TiCu, Ti_2Cu, $TiCu_4$, Cu(ss), Ti(ss) and Mo phases. The diffusion and dissolution of Mo from the molybdenum substrate to the brazing region occur during the brazing process for both joints.

(2) For the molybdenum/tungsten joint, the thickness of the brazing region is about 150 μm. No diffusion or dissolution takes place between the Cu78Ti22 filler and the tungsten substrate. However, the absorption of Ti on the tungsten side promotes interfacial bonding between the brazing region and the tungsten substrate. For the molybdenum/graphite joint, the brazing region exhibits a thickness of about 110 μm, which is less than that of the molybdenum/tungsten joint. This may be due to the penetration of the molten filler into the porous graphite. The active Ti in the filler reacts with the graphite to form a TiC layer with a thickness of 200~300 nm at the brazing region/graphite interface, which contributes to the interfacial bonding of the filler with the graphite.

(3) The molybdenum/tungsten and molybdenum/graphite joints exhibit shear strengths of 51.4 ± 7.3 MPa and 12.3 ± 3.2 MPa, respectively. Fracture of the molybdenum/tungsten joint after the shear test occurs at the brazing region/tungsten interface, mainly because of the relatively weak interfacial bonding. The molybdenum/graphite joint breaks on the graphite side near the brazing region, which is caused mainly by the large residual stress in the joint.

Authors' contributions: Longkun Huang: Investigation, Methodology, Writing-original draft; Siyu Miao: Investigation, Data curation ; Yingjie Zeng: Investigation, Validation; Yuqi Cai: Investigation; Julfikar Haider: Writing- review & editing; Yangwu Mao: Conceptualization, Resources, Figure arrangement, Supervision, Writing- review & editing

Funding This work was supported by the WIT Graduate Education Innovation Fund (Grant No. CX2021164).

Data Availability All data during the study are available from the corresponding author by request.

Declarations

Conflict of interest The authors declare no competing interests.

References

1. Chen YH, Zhang RH, Hao ZH, Shu YC, He JL (2023) Study on reduction of MoO_2 by carbon diffusion to prepare molybdenum powder. Mater Today Commun 35:105643. https://doi.org/10.1016/j.mtcomm.2023.105643.
2. Xu B, Cai YQ, Haider J, Khan FN, Shehbaz T, Zhao HY, Mao YW (2023) Microstructural and mechanical characterizations of Mo/W and Mo/Graphite joints with BNi2 paste. Adv Eng Mater 26:2301004. https://doi.org/10.1002/adem.202301004.
3. Fedotov I, Suchkov A, Sliva A, Dzhumaev P, Kozlov I, Svetogorov R, Bachurina D, Sevryukov O (2021) Study of the microstructure and thermomechanical properties of Mo/graphite joint brazed with Ti-Zr-Nb-Be powder filler metal. J Mater Sci 56:11557-11568. https://doi.org/10.1007/s10853-021-06015-9.
4. Yao Q, Cheng HC, Fan JL, Yan HX. Zhang CG (2019) High strength Mo/Ti6Al4V diffusion bonding joints: Interfacial microstructure and mechanical properties. Int J Refract Met Hard Mater 82:159-166. https://doi.org/10.1016/j.ijrmhm.2019.04.009.
5. Chatterjee A, Kumar S, Tewari R, Dey GK (2016) Welding of Mo-based alloy using electron beam and laser-GTAW hybrid welding techniques. Metall Mat Trans A 47:1143-1152. https://doi.org/10.1007/s11661-015-3267-8.
6. Zhang LJ, Ma RY, Zhang YB, Guo Q, Wang CH, Zhang JX, Na SJ (2020) Investigation on dissimilar laser beam welding of molybdenum to zirconium via pure titanium interlayer. Opt Laser Technol 131:106327. https://doi.org/10.1016/j.optlastec.2020.106327
7. Dong LL, Chen WG, Hou LT, Wang JJ, Song JL (2017) Metallurgical and mechanical examinations of molybdenum/graphite joints by vacuum arc pressure brazing using Ti-Zr filler materials. J Mater Process Technol 249:39-45. https://doi.org/10.1016/j.jmatprotec.2017.06.007.
8. Min M, Mao YW, Deng QR, Wang GM, Wang SG (2020) Vacuum brazing of Mo to 316L stainless steel using BNi-2 paste and Cu interlayer. Vacuum 175:109282. https://doi.org/10.1016/j.vacuum.2020.109282.
9. Wang C, Fu QG, Zhou L, Ma YF, Sun J, Zhang JP (2021) Improved mechanical strength of the C/C–Mo joints by introducing MoNiSi ternary compounds as the main phase of the interlayer. Mater Sci Eng A 819:141502. https://doi.org/10.1016/j.msea.2021.141502.
10. Sene FF, Motta CC (2013) Synthesis and characterization of Ni-Mo filler brazing alloy for Mo-W joining for microwave tube technology. Mater Res 16:417-423. https://doi.org/10.1590/S1516-14392013005000019.

11. Fedotov I, Suchkov A, Sliva A, Dzhumaev P, Kozlov I, Svetogorov R, Sevryukov O (2021) Simulated thermal tests of a molybdenum/graphite X-ray target manufactured with a novel Ti-Zr-Nb-Be powder filler metal: an investigation of the brazed joint evolution under operating conditions. J Manuf Process 69:142-151. https://doi.org/10.1016/j.jmapro.2021.07.035.
12. Liu DG, Zou JX, Zhang P, Zhou SW, Liu H, Li ZQ (2023) Effect of Ti–Cr filler on microstructure, mechanical properties, and thermal shock resistance of TZM/graphite brazed joints. Int J Refract Met Hard Mater 115:106310. https://doi.org/10.1016/j.ijrmhm.2023.106310.
13. Lu QB, Long WM, Zhong SJ, Qin J, Jiu YT, Sun HW (2020) TZM/graphite interface behavior in high-temperature brazing by Ti-based brazing filler materials. Weld World 64:1877-1885. https://doi.org/10.1007/s40194-020-00967-3.
14. Lin CC, Shu CH, Chen C, Shiue RK, Shy HJ (2012) Brazing porous tungsten and molybdenum using palladium and titanium foils. Int J Refract Met Hard Mater 31:284-287. https://doi.org/10.1016/j.ijrmhm.2011.10.007.
15. Feng HL, Chen B, Ren HS, Xiong HP, Li WW, Cheng YY, Zhou WJ (2020) Joining SiC ceramic and metal Mo with AuPdCoMnNi alloy and interfacial reactions. Weld World 64: 1771-1778. https://doi.org/10.1007/s40194-020-00956-6
16. Lin DY, Chen Q, Xu JX, Hu SP, Bian H, Fu W, Song YY, Lu YX, Song XG (2024) Microstructure evolution and mechanical properties of SiC/Mo joint brazed with FeCoCrNi high-entropy alloy filler. Ceram Int 50: 42045-42058. https://doi.org/10.1016/j.ceramint.2024.08.048
17. Kang YH, Feng KM, Zhang WT, Mao YW (2021) Microstructural and mechanical properties of CFC composite/Ti6Al4V joints brazed with Ag-Cu-Ti and refractory metal foils. Arch Civ Mech Eng. 21:113. https://doi.org/10.1007/s43452-021-00268-6.
18. Farzad H and Ahad S (2023) Interfacial reactions in actively brazed Cu-Al_2O_3 composites and copper using a newly developed Cu-Sn-Ag-Ti filler alloy. Sci Technol Weld Joining 28: 444-454. https://doi.org/10.1080/13621718.2023.2173878
19. Okamoto H, Schlesinger ME and Mueller EM (2016) ASM Handbook Volume 3: Alloy Phase Diagrams. Ohio(OH), ASM International
20. Duan Y, Mao YW, Xu ZM, Deng QR, Wang GM, Wang SG (2019) Joining of graphite to Ti6Al4V alloy using Cu-based fillers. Adv Eng Mater 21: 1900719. https://doi.org/10.1002/adem.201900719

21. Liu MG, Bai L, Deng YQ (2021) Strong Mo/Cu interfacial bonding facilitated by consumable Ti interlayer. J Manuf Process 74:136-140. https://doi.org/10.1016/j.jmapro.2021.12.010.

22. Lin CC, Chen C, Shiue RK, Shi SC (2011) Vacuum brazing Mo using Ti-Ni-Nb braze alloys. Int J Refract Met Hard Mater 29:641-644. https://doi.org/10.1016/j.ijrmhm.2011.04.003.

23. Peng LX, Mao YW, Zhang YZ, Xi LX, Deng QR (2018) Microstructural and mechanical characterizations of W/CuCrZr and W/steel joints brazed with Cu-22TiH_2 filler. J Mater Process Technol 254:346-352. https://doi.org/10.1016/j.jmatprotec.2017.11.056.

24. Yu J, Miao XL, Zhang HT, Wang B, Qu CM (2022) The effect of Ti content in the filler powder on interfacial microstructure and mechanical properties of C/C composites/T2-Copper joints via thermo-compensated resistance brazing welding. Metals 12 (5):815. https://doi.org/10.3390/met12050815.

25. Mao YW, Yu S, Zhang YZ, Guo BB, Ma ZB, Deng QR (2015) Microstructure analysis of graphite/Cu joints brazed with (Cu-50TiH_2) + B composite filler. Fusion Eng Des 100:152-158. https://doi.org/10.1016/j.fusengdes.2015.05.011.

26. Izaguirre I, de Prado J, Sánchez M, Ruiz A, Ureña A (2024) Wettability and microstructural evolution of copper filler in W and EUROFER brazed joints. Int J Adv Manuf Technol 131:5905-5921. https://doi.org/10.1007/s00170-024-13338-9.

27. de Prado J, Sánchez M, Ureña A (2016) Development of brazing process for W-Eurofer joints using Cu-based fillers. Phys Scr T167:014022. https://doi.org/10.1088/0031-8949/T167/1/014022.

28. Shang JL, Yan JZ, Li N (2014) Brazing W and Fe-Ni-Co alloy using Ag–28Cu and Ag-27Cu-3.5Ti fillers. J Alloys Compd 611:91-95. https://doi.org/10.1016/j.jallcom.2014.05.106.

29. Shao HK, Wu AP, Bao YD, Zhao Y, Zou GS, Liu L (2018) Novel transient liquid phase bonding through capillary action for high-temperature power devices packaging. Mater Sci Eng A 724:231-238. https://doi.org/10.1016/j.msea.2018.03.097.

30. Vidyuk TM, Dudina DV, Esikov MA, Mali VI, Anisimov AG, Bokhonov BB, Batraev IS (2022) Pulsed current-assisted joining of copper to graphite using Ti-Cu brazing layers. Mater Today Proc 25:377-380. https://doi.org/10.1016/j.matpr.2019.12.095.

31. Song XR, Li HJ, Zeng XR (2016) Brazing of C/C composites to Ti6Al4V using multiwall carbon nanotubes reinforced TiCuZrNi brazing alloy. J Alloys Compd 664:175-180. https://doi.org/10.1016/j.jallcom.2015.12.242.

32. Shi JM, Zhang LX, Chang Q, Sun Z, Feng JC, Ma N (2018) Improving the strength of the ZrC-SiC and TC4 brazed joint through fabricating graded double layered composite structure on TC4 surface. Metall Mat Trans B 49:902-911. https://doi.org/10.1007/s11663-018-1253-4.
33. Zhou XW, Huang YD, Chen YH, Peng P (2018) Laser joining of Mo and Ta sheets with Ti6Al4V or Ni filler. Opt Laser Technol 106:487-494. https://doi.org/10.1016/j.optlastec.2018.05.004.
34. Manikandan P, Lee JO, Mizumachi K, Mori A. Raghukandan K, Hokamoto K (2011) Underwater explosive welding of thin tungsten foils and copper. J Nucl Mater 418:281-285. https://doi.org/10.1016/j.jnucmat.2011.07.013.
35. Bonk S, Reiser J, Hoffmann J, Hoffmann A (2016) Cold rolled tungsten (W) plates and foils: Evolution of the microstructure. Int J Refract Met Hard Mater 60:92-98. https://doi.org/10.1016/j.ijrmhm.2016.06.020.
36. Chu QL, Zhang M, Li JH, Fan QY, Xie WW, Bi ZY (2015) Joining of Cp-Ti/Q345 sheets by Cu-based filler metal and effect on interface. J Mater process Technol 225:67-76. https://doi.org/10.1016/j.jmatprotec.2015.05.017.
37. Zong WA, Zhang S, Zhang CH, Ren L, Wang Q (2020) Design and characterization of selective laser-melted Ti6Al4V-5Cu alloy for dental implants. Mater Corros 71:1697-1710. https://doi.org/10.1002/maco.202011650.
38. Konieczny M (2008) Processing and microstructural characterisation of laminated Ti-intermetallic composites synthesised using Ti and Cu foils. Mater Lett 62:2600-2602. https://doi.org/10.1016/j.matlet.2007.12.067.
39. de Prado J, Sánchez M, Ureña A (2017) Improvements in W-Eurofer first wall brazed joint using alloyed powders fillers. Fusion Eng Des 124:1082-1085. https://doi.org/10.1016/j.fusengdes.2017.03.126.
40. de Prado J, Sánchez M, Ureña A (2017) Evaluation of mechanically alloyed Cu-based powders as filler alloy for brazing tungsten to a reduced activation ferritic-martensitic steel. J Nucl Mater 490:188-196. https://doi.org/10.1016/j.jnucmat.2017.04.033.
41. Apblett C, Ficalora PJ (1991) Stress generation in thin Cu-Ti films in vacuum and hydrogen. J Appl Phys 69:4431-4432. https://doi.org/10.1063/1.348370.
42. Cai YQ, Xu B, Ma XJ, Haider J, Mao YW, Wang SG (2023) Bonding of graphite to Cu with metal multi foils. Arch Civ Mech Eng 23:58. https://doi.org/10.1007/s43452-023-00603-z.

43. Xing LL, Lin JC, Huang M, Yang WQ (2019) Joining of graphite to copper with Nb interlayer: microstructure and mechanical properties. Adv Eng Mater 21:1800810. https://doi.org/10.1002/adem.201800810.